

Python Program for 3D Linear Dynamic Reticular Structural Analysis Based on Finite Element Method

Gabriel C. Ferreira, Maria S. M. Sampaio

*Dept. of Civil Engineering, University of Amazonas State
Darcy Vargas Avenue, 69050-020, Amazonas/Manaus, Brazil
gcarva.ferreira@gmail.com, msampaio@uea.edu.br*

Abstract. Dynamic structural analysis in civil engineering is the method, in which, the vibrations response, modes, frequencies, displacements, velocities and accelerations, of a real-world structure caused by arbitrary external excitements is predicted, before its design and construction. But even for simple structures, to conceive the analysis by hand, without relying on simplifications, for which, by themselves, sacrifices precision of the analytical solutions, is hard. Therefore, a computational method to solve these structures is needed. But these softwares come at a high monetary cost, causing an inaccessibility for students to have access to, even for confirming and/or learning purposes. For such, a computational tool development, capable of linear structural analysis, both in 2D and 3D, in dynamic regime, open-source for all, were proposed. To make it possible, the Finite Element Method (FEM), for structural discretization, the Rayleigh damping model, for viscous approximation, the Newmark's numerical method, for vibration analysis, and the Eigen-vectors and values, for modal analysis, and Python, for the programming language, were used. And to a reticular structures, they were applied. Then, with examples found in the available literature in the subject of dynamic structural analysis, were tested and compared. The results from examples tested, errors ranging from 10^{-5} to 10^{-2} were shown by the tool, in the same unit as the mesh and properties and time discretization, inputted in the program, compared to examples available in the literature.

Keywords: linear dynamic analysis, finite element method, Newmark's method, python language.

1 Introduction

As Steven Strogatz said "since Newton, mankind has come to realize that the laws of physics are always expressed in the language of differential equations". And in engineering is not different, since the field applies the understanding of such laws into real-world structures. But, in some structures, the complexity of these real-world structures are so great, that it falls off where the knowledge hits its edge. For such structures, a CAE is needed to attain an approximate solution to such.

CAE, Computer Aided Engineering, is the appliance of the computer processing power, greatly increasing engineers capability to predict its behavior. But to harness such power, in such complex problems, an advanced numerical method is imperative, for a computer does not work at a continuum, but at the discrete. Advanced numerical methods, for which finite element methods are the most efficient and most frequently used, are extremely important for complicated engineering structures such as spacecraft, buildings, bridges, dams, etc. By means of dynamic analyses and simulations one can determine whether a structure under considerations will fulfill its function, and the results of the dynamic loadings acting on this structure can be predicted, Mackerle [1].

The Finite Element Method, FEM for short, is a method in which the structure is discretized into elements with finite size, connected through nodes, Zienkiewicz and Taylor [2] and Oden and Reddy [4], in the bidimensional case with 6 degrees of freedom (d.o.f.), being 3 for each node, and in the tridimensional case 12 d.o.f., 6 for each. In which, through matrices, element-type (reticle in this paper), is approximated (through polynomials in this paper, with Euler-Bernoulli assumptions), inputting values relevant to the specific properties, that is allocated into a global matrix, that then describes the structure as a whole. These element-wise matrices, were derived through energy method, applying the stationary-action principle. The kinetic energy equations were used to derive the mass matrix, while the potential elastic energy equation were used in the stiffness matrix. The degree of the polynomials coincides with the d.o.f. involvements with each other, degree 4 for shear and momentum (2 d.o.f per node), degree 2 for axial (1 d.o.f. per node) as well for torsion, Weaver and Gere [5] and, Weaver and Johnston [6].

Finally, there are many computational tools for structural analysis, usually available in commercial version. Therefore, the purpose of this paper is to develop a free and open-source computational tool for structural analysis. For such, it was written with Python as language, known for its accessibility.

2 Finite Element Formulation for 3D Reticular Linear Dynamic Analysis

So, let a frame finite element of length (L), area (A), density (ρ), Young modulus (E), shear modulus (G) and inertial moments (I_x , I_y and I_z) be subjected to a linearly distributed load $q(x)$. Since, by hypothesis, the frame is subjected to axial forces, bending forces and torsion, the nodal parameters associated with nodes i and j of this finite element are rotations and translations as shown in Fig. 1.

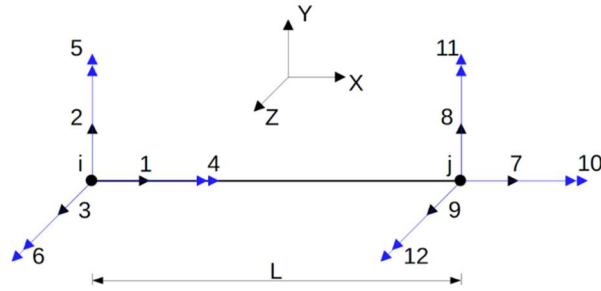


Figure 1. Finite element nodal degrees of freedom.

For such element type, with linear assumptions, to treat the d.o.f. as separate groups, since the superposition principle applies, is possible into two groups: pair and sole. There are two pairs, where the relationship between shear force and its momentum are related (2 and 6 in i with 8 and 12 in j , for example). And there are two sole, like torsion (4 in i and 10 in j) and axial force (1 in i and 7 in j), where only one d.o.f. from each side is involved. The polynomials degrees coincide with the d.o.f.s involved, and then the polynomials with its coefficients attained from boundary conditions, allocated into a single matrix, super positioned. That's how the reticular element-type is described. And then each element, will have its particular properties described by its length, density, area, etc.

3 Dynamic Analysis

According to Rao [7], the dynamic equilibrium is given by Eq. (1).

$$\mathbf{M}\ddot{\vec{X}}(t) + \mathbf{C}\dot{\vec{X}}(t) + \mathbf{K}\vec{X}(t) = \vec{F}(t) \quad (1)$$

where, \mathbf{M} is the mass matrix, \mathbf{C} is the damping matrix, \mathbf{K} is the stiffness matrix, $\ddot{\vec{X}}(t)$ is the accelerations vector, $\dot{\vec{X}}(t)$ is the velocities vector, $\vec{X}(t)$ is the displacements vector and $F(t)$ is the forces vector.

In the dynamic case, the element is represented by both, the mass and the stiffness matrices as shown in Eq. (3) and (4), respectively. For the damping matrix, the Rayleigh method was used, Paz and Leigh [8]. The Rayleigh method is an approximation by a linear junction of both matrices (mass and stiffness), each with weight coefficients. And its models the loss of energy from the system through time.

3.1 Tridimensional Stiffness Matrix and Consistent Mass Matrix

With twelve d.o.f., as show in Fig. 1, each consistent matrix will be a 12x12, in the local coordinate system. Since the derivation from the energy equations to the matrix are non-trivial, the consistent mass and stiffness matrices are only shown, as we can see in Eq. (2)-(3), respectively.

$$\mathbf{K} = \begin{bmatrix} \frac{EA}{L} & 0 & 0 & 0 & 0 & 0 & -\frac{EA}{L} & 0 & 0 & 0 & 0 & 0 \\ 0 & \frac{12EI_z}{L^3} & 0 & 0 & 0 & \frac{6EI_z}{L^2} & 0 & -\frac{12EI_z}{L^3} & 0 & 0 & 0 & \frac{6EI_z}{L^2} \\ 0 & 0 & \frac{12EI_y}{L^3} & 0 & -\frac{6EI_y}{L^2} & 0 & 0 & 0 & -\frac{12EI_y}{L^3} & 0 & -\frac{6EI_y}{L^2} & 0 \\ 0 & 0 & 0 & \frac{GI_x}{L} & 0 & 0 & 0 & 0 & 0 & -\frac{GI_x}{L} & 0 & 0 \\ 0 & 0 & -\frac{6EI_y}{L^2} & 0 & \frac{4EI_y}{L} & 0 & 0 & 0 & \frac{6EI_y}{L^2} & 0 & \frac{2EI_y}{L} & 0 \\ 0 & \frac{6EI_z}{L^2} & 0 & 0 & 0 & \frac{4EI_z}{L} & 0 & -\frac{6EI_z}{L^2} & 0 & 0 & 0 & \frac{2EI_z}{L} \\ -\frac{EA}{L} & 0 & 0 & 0 & 0 & 0 & \frac{EA}{L} & 0 & 0 & 0 & 0 & 0 \\ 0 & -\frac{12EI_z}{L^3} & 0 & 0 & 0 & -\frac{6EI_z}{L^2} & 0 & \frac{12EI_z}{L^3} & 0 & 0 & 0 & -\frac{6EI_z}{L^2} \\ 0 & 0 & -\frac{12EI_y}{L^3} & 0 & \frac{6EI_y}{L^2} & 0 & 0 & 0 & \frac{12EI_y}{L^3} & 0 & \frac{6EI_y}{L^2} & 0 \\ 0 & 0 & 0 & -\frac{GI_x}{L} & 0 & 0 & 0 & 0 & 0 & \frac{GI_x}{L} & 0 & 0 \\ 0 & 0 & -\frac{6EI_y}{L^2} & 0 & \frac{2EI_y}{L} & 0 & 0 & 0 & \frac{6EI_y}{L^2} & 0 & \frac{4EI_y}{L} & 0 \\ 0 & \frac{6EI_z}{L^2} & 0 & 0 & 0 & \frac{2EI_z}{L} & 0 & -\frac{6EI_z}{L^2} & 0 & 0 & 0 & \frac{4EI_z}{L} \end{bmatrix} \quad (2)$$

$$\mathbf{M} = \frac{\rho L}{420} \begin{bmatrix} 140A & 0 & 0 & 0 & 0 & 0 & 70A & 0 & 0 & 0 & 0 & 0 \\ 0 & 156A & 0 & 0 & 0 & 22LA & 0 & 54A & 0 & 0 & 0 & -13LA \\ 0 & 0 & 156A & 0 & -22LA & 0 & 0 & 0 & 54A & 0 & +13LA & 0 \\ 0 & 0 & 0 & 140J & 0 & 0 & 0 & 0 & 0 & 70J & 0 & 0 \\ 0 & 0 & -22LA & 0 & 4L^2A & 0 & 0 & 0 & -13LA & 0 & -3L^2A & 0 \\ 0 & 22LA & 0 & 0 & 0 & 4L^2A & 0 & 13LA & 0 & 0 & 0 & -3L^2A \\ 70A & 0 & 0 & 0 & 0 & 0 & 140A & 0 & 0 & 0 & 0 & 0 \\ 0 & 54A & 0 & 0 & 0 & 13LA & 0 & 156A & 0 & 0 & 0 & -22LA \\ 0 & 0 & 54A & 0 & -13LA & 0 & 0 & 0 & 156A & 0 & +22LA & 0 \\ 0 & 0 & 0 & 70J & 0 & 0 & 0 & 0 & 0 & 140J & 0 & 0 \\ 0 & 0 & +13LA & 0 & -3L^2A & 0 & 0 & 0 & +22LA & 0 & 4L^2A & 0 \\ 0 & -13LA & 0 & 0 & 0 & -3L^2A & 0 & -22LA & 0 & 0 & 0 & 4L^2A \end{bmatrix} \quad (3)$$

According to Cook et al [9], the use of a consistent mass matrix results in greater accuracy despite lower computational savings compared to the discrete mass matrix. The use of this consistent mass matrix is important when implicit temporal integration algorithms are employed.

3.2 Newmark β

As for the time discretization, the Newmark's method were used, Petyt [10]. It's given by a Taylor expansion from the displacements given a time t into a time $t+1$, as shown in Eq. (4). Which is then considered that the acceleration between these two points of time, is the average between the two, which gives $\beta = 0.25$ and $\gamma = 0.5$.

$$u_{t+1} = u_t + \Delta t \dot{u}_t + \Delta t^2 \left[\left(\frac{1}{2} - \beta \right) \ddot{u}_t + \beta \ddot{u}_{t+1} \right] \quad \text{and} \quad \dot{u}_{t+1} = \dot{u}_t + \Delta t \{ (1-\gamma) \ddot{u}_t + \gamma \ddot{u}_{t+1} \} \quad (4)$$

Then, the R and Q parameters are derived from it, as shown in Eq. (5), respectively:

$$R = \dot{u}_t + \Delta t (1-\gamma) \ddot{u}_t \quad \text{and} \quad Q = \frac{u_t}{\beta \Delta t^2} + \frac{\dot{u}_t}{\beta \Delta t} + \left(\frac{1}{2} - \beta \right) \ddot{u}_t \quad (5)$$

Finally, those parameters were applied into the Eq. (1). Turning a continuum equation that depends on displacement, velocity and acceleration, into one that only depends into past information, through R and Q, and the displacements the only unknown, as shown in Eq. (6).

$$\left(\frac{\mathbf{M}}{\beta\Delta t^2} + \frac{\mathbf{C}\gamma}{\beta\Delta t} + \mathbf{K} \right) u_{t+1} = F - \mathbf{M}Q_t - \mathbf{C}R_t - \mathbf{C}Q_t\gamma\Delta t \quad (6)$$

4 Numerical Results and Validation

Analytical and numerical examples available in the literature were tested and the obtained results showed the good performance of the implemented tool for the tested examples. In this section, three examples are presented.

4.1 Cantilever beam under harmonic force presented by Torii [11]

The problem consists of a classical cantilever beam in bidimensional space, with length of $L = 1$ m as shown in Fig. 2. The geometric and material properties are unitary, and the time span of the analysis is $T = 10$ s, with a time-step of $\Delta T = 0.00125$ s. A unitary senoidal force in the X direction, with angular frequency of $\omega = 20$ rad/s, with no phase shift, is applied. Figs. 3-6 compares the analytical solution given in Torii [11] with the present numerical solution for different discretizations. Black-line is the analytical solution and blue-line is the present numerical solution. As it is possible to observe the numerical solution converges to the analytical solution as the number of finite elements of the discretization increases.



Figure 2. Cantilever beam under harmonic force, Torii [11].

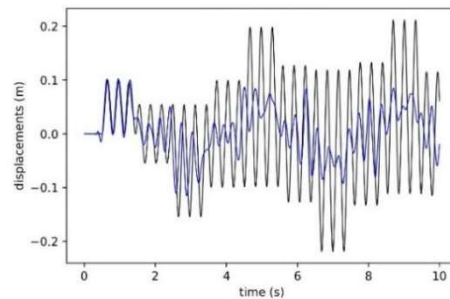


Figure 3. Numerical solution with 20 elements.

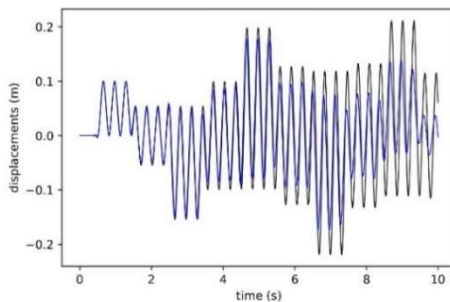


Figure 4. Numerical solution with 50 elements.

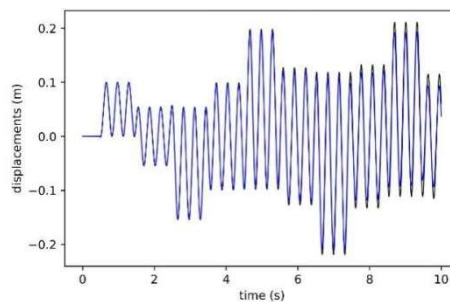


Figure 5. Numerical solution with 100 elements.

4.2 3D Frame under variable force presented by Barros [12].

The next two examples comes from Barros [12]. Both have an pulse as dynamical forces (Fig. 7), although the P value vary, the pulse time span in constant with duration of $T = 0.04$ s and its peak value at $t_1 = 0.02$ s, starting at $t = 0$, as well as its direction through positive X.

The first 3D example, is a frame with 5 nodes, labeled from 1 to 5 as shown in Fig. 6. The nodes 2 to 5 are constrained in all d.o.f.. The element properties are as follows in Table 1. All bars have been refined, so that each bar has 2 elements. And the time step of $\Delta t = 10^{-3}$ s was used. The results are as follows in Fig. 8 in a qualitative comparison with the reference solution shown in Fig. 9. It was not possible to find the value of P applied.

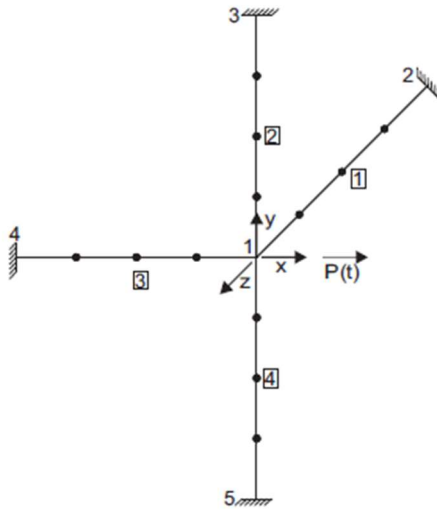


Figure 6 – 3D Frame under horizontal pulse load, Barros [12].

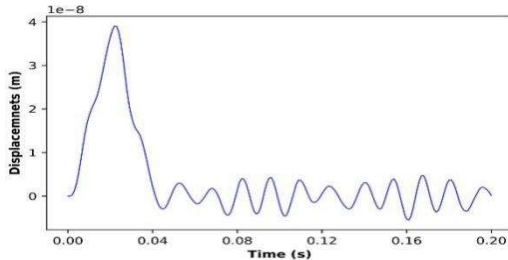


Figure 8 – Present solution for $P = 50$ N.

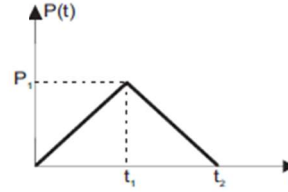


Figure 7 – Impulsive excitation, Barros [12].

Table 1 – Material and geometrical properties.

Properties	Bars 1 and 3	Bars 2 and 4
E (N/m)	207×10^9	207×10^9
G (N/m)	80×10^9	80×10^9
ρ (kg/m ³)	43530.56	38840.53
A (m ²)	3.23×10^{-2}	1.81×10^{-2}
J (m ⁴)	1.66×10^{-5}	5.33×10^{-6}
I_x (m ⁴)	8.32×10^{-5}	2.66×10^{-5}
I_z (m ⁴)	8.32×10^{-5}	2.66×10^{-5}

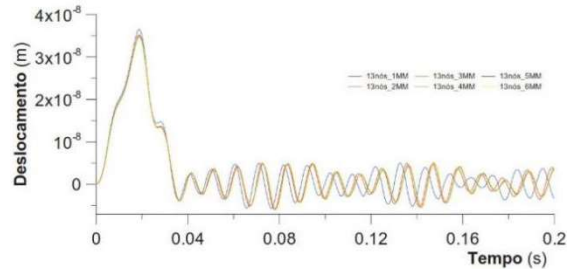


Figure 9 – Reference solution, Barros [12].

4.3 Two floors 3D Frame under variable force presented by Barros [12]

The second 3D example is a two floors high frame structure, without slabs (Fig. 10), with 2 types of cross sections. The pillars, or bars in the Z direction, have section AA, while the beams have section BB (Table 2). They both have $E = 219,9 \times 10^9$ N/m, $G = 87,96 \times 10^9$ N/m and $\rho = 7850$ kg/m³. All bars have been refined, so that each bar has 2 elements. And the time step of $\Delta t = 10^{-5}$ s was used. The results are as follows in Fig. 11 in a qualitative comparison with reference solution shown in Fig. 12. Again, it was not possible to find the value of P applied.

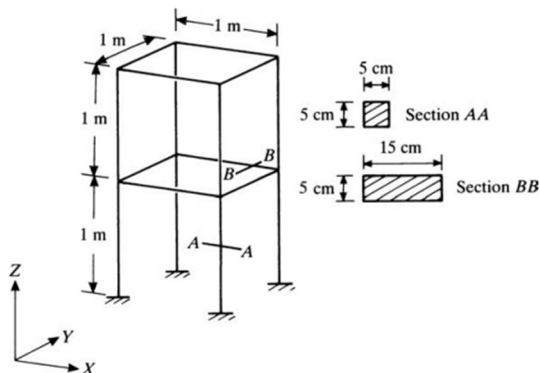


Figure 10 – Geometry of the framework, Petyt [10].

Table 2 – Material and geometrical properties.

Properties	Section AA	Section BB
A (m ²)	2.5×10^{-3}	7.5×10^{-3}
J (m ⁴)	1.04×10^{-6}	1.67×10^{-5}
I_y (m ⁴)	5.21×10^{-7}	1.41×10^{-5}
I_z (m ⁴)	5.21×10^{-7}	1.56×10^{-6}

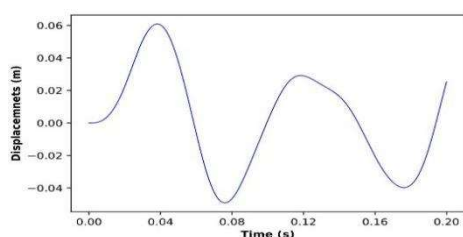


Figure 11 – Present solution for $P = 75000$ N.

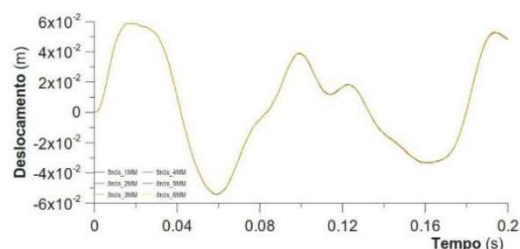


Figure 12 – Reference solution, Barros [12].

5 Conclusions

A 3D finite element formulation in dynamic regime, in Python language, for the reticular structural linear analysis, was successfully implemented as it is possible to conclude from the obtained results. It is important to mention that in this first moment the focus was on the development of the first functions of the program, that is, the development of a tool for the analysis of reticular structures in a linear elastic regime. Future works will aim to develop a graphical interface that will enable a more user-friendly environment for input data, currently done through a text file or directly in the programming environment. It concludes, with a free and open-source Python computation code, open for all to use, and such, the foundations for future engineers to further expand its functionalities is available. The source code is available in the GitHub repository under GNU v3 license. The GitHub link being: <https://github.com/gCarvalhoFerreira/FEM-Python>.

Acknowledgements. The authors would like to thank the State of Amazonas Research Support Foundation (FAPEAM) for the financial support granted through the Scientific Initiation Program (PAIC): 2022-2023 Edition/SISPROJ Project Number 37452.

Authorship statement. The authors hereby confirm that they are the sole liable persons responsible for the authorship of this work, and that all material that has been herein included as part of the present paper is either the property (and authorship) of the authors, or has the permission of the owners to be included here.

References

- [1] J. Mackerle, Finite element vibration and dynamic response analysis of engineering structures: a bibliography.
- [2] O. C. Zienkiewicz and R. L. Taylor, *The Finite Element Method: Basic Formulation and Linear Problems*, 4th Edition, vol. 1. McGraw-Hill, 1989.
- [3] T.J.R. Hughes, *The Finite Element Method – linear static and dynamic finite element analysis*. Prentice-Hall International, Inc. Englewood Cliffs, New Jersey, 1987.
- [4] J.T. Oden and J.N. Reddy, *An introduction to the mathematical theory of finite elements*. John Wiley & Sons, New York, 1976.
- [5] W. Weaver and J.M. Gere, *Matrix Analysis of Framed Structures – 3rd Edition*. New York: Van Nostrand Reinhold, 1990.
- [6] W. Weaver and P.R. Johnston, *Structural Dynamics by Finite Elements*. New Jersey: Prentice-Hall, INC. Englewood Cliffs, 1987.
- [7] S.S. RAO, *Mechanical vibration*. 5nd. ed., Pearson Prentice Hall, 2008.
- [8] M. Paz and W. Leigh, *Structural Dynamics: Theory and Computation*. 5th Edition, Springer S., New York, 2004.
- [9] R. D. Cook, et al. *Concepts and applications of finite element analysis*. 4. ed. New York. John Wiley & Sons, 1989.
- [10] M. Petyt. *Introduction to Finite Element Vibration Analysis*. Cambridge, 2010.
- [11] A. J. Torii, Análises dinâmicas de estruturas com o método dos elementos finitos generalizado. 2012. 223 f. PhD thesis, Universidade Federal do Paraná, Curitiba, 2012.
- [12] Barros, R. N., Análise dinâmica de treliças e pórticos tridimensionais usando uma técnica avançada de superposição modal. Dissertation (Masters in Civil Engineering), Pontífice Universidade Católica do Rio de Janeiro, 2017.